ACS Chemical Neuroscience

pubs.acs.org/chemneuro Research Article

Multivariate Machine Learning Analyses in Identification of Major Depressive Disorder Using Resting-State Functional Connectivity: A Multicentral Study

Yachen Shi, Linhai Zhang, Zan Wang, Xiang Lu, Tao Wang, Deyu Zhou,* and Zhijun Zhang*

Cite This: *ACS Chem. Neurosci.* 2021, 12, 2878−2886 Read Online

ACCESS | Metrics & More | Article Recommendations | Supporting Information

ABSTRACT: Diagnosis of major depressive disorder (MDD) using resting-state functional connectivity (rs-FC) data faces many challenges, such as the high dimensionality, small samples, and individual difference. To assess the clinical value of rs-FC in MDD and identify the potential rs-FC machine learning (ML) model for the individualized diagnosis of MDD, based on the rs-FC data, a progressive three-step ML analysis was performed, including six different ML algorithms and two dimension reduction methods, to investigate the classification performance of ML model in a multicentral, large sample dataset [1021 MDD patients and 1100 normal controls (NCs)]. Furthermore, the linear least-squares fitted regression model was used to assess the relationships between rs-FC features and the severity of clinical symptoms in MDD patients. Among used ML methods, the rs-FC model constructed by the eXtreme Gradient Boosting (XGBoost) method showed the optimal classification performance for distinguishing MDD patients from NCs at the individual level (accuracy = 0.728, sensitivity = 0.720, specificity = 0.739, area under the curve = 0.831). Meanwhile, identified rs-FCs by the XGBoost model were primarily distributed within and between the default mode network, limbic network, and visual network. More importantly, the 17 item individual Hamilton Depression Scale scores of MDD patients can be accurately predicted using rs-FC features identified by the XGBoost model (adjusted R^2 = 0.180, root mean squared error = 0.946). The XGBoost model using rs-FCs showed the optimal classification performance between MDD patients and HCs, with the good generalization and neuroscientifical interpretability.

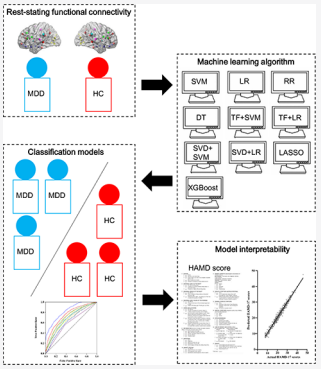

KEYWORDS: *Major depressive disorder, resting-state functional connectivity, multiple-center, machine learning, classification, eXtreme Gradient Boosting*

INTRODUCTION

Major depressive disorder (MDD) is the most common of the severe psychiatric diseases and the primary cause of disability worldwide.[1] Until now, the pathophysiology of MDD has been understood considerably and various hypotheses have been proposed, such as the monoamine hypothesis, hypothalamic−pituitary−adrenal axis changes, inflammation, and neuroplasticity, but there is no single mechanism can completely elucidate total aspects of the disease.[2] Likewise, none of universally accepted objective biomarkers are used for the clinical diagnosis of MDD so far, although some indicators show great potential, e.g., brain derived neurotrophic factor.[3] Additionally, the misdiagnosis of MDD is one of the main reasons for the poor treatment response of the antidepressant.[4] Therefore, it is crucial to improve the diagnostic accuracy of MDD in the clinic.

Advances in technology have made it possible to understand the brain structure and function through neuroimaging; in particular, the application of magnetic resonance imaging (MRI) has important implications for the MDD study.[5] Functional MRI (fMRI) can provide some useful information about the brain functional connectivity (FC) involved in the latent mechanism of MDD, e.g., the depressive emotion regulation and impaired reward circuits related to anhedonia.[6] Our previous study revealed that MDD patients had significantly decreased reward network connectivity within the prefrontal-striatal regions.[7] Furthermore, Chen et al. found that the functional dysconnectivity within prefrontal-limbic and prefrontal-striatum systems might be relevant to the dysregulation of negative and positive emotion processing in MDD patients, respectively.[8] However, the changes of whole-brain FCs identified in MDD patients are associated with the heterogeneous clinical presentation, which results in the difficulty of replicating these findings by different research groups. Meanwhile, studies on the brain FCs as effective biomarkers have been largely based on the group-level rather than individual statistics, which has limited utility in the clinical diagnosis of MDD.

Received: April 21, 2021
Accepted: June 16, 2021
Published: July 20, 2021

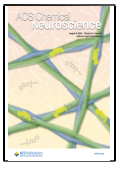

https://doi.org/10.1021/acschemneuro.1c00256
ACS Chem. Neurosci. 2021, 12, 2878−2886

Machine learning (ML) is capable of generalizing patterns from the input data to generate a classification on new data and has been widely used to build classifiers for the individual diagnosis of MDD based on MRI-related data. For resting-state FC (rs-FC) data, previous studies showed multiple classifiers with the most accuracy (95%) for diagnosing MDD (Table S1). However, these results need to be treated with caution due to the sample sizes of these studies being fairly small. Furthermore, a considerable hurdle of neuroimaging data is high dimensionality, which raises an open question about which ML algorithms is favorable for an rs-FC data based classification. Although some previous studies had performed multiple feature selection methods combined with the Support Vector Machine (SVM) or one feature selection method combine with multiple classification algorithms to build models,[9−12] these results were limited in their exploration of ML methods, especially ensemble methods.[13] Therefore, a systematic investigation among different ML strategies is necessary, which can provide instructive insights for building a MDD classification model based on the rs-FC data.

The aims of the present study are to assess the potential clinical value of rs-FC and to identify the optimal multivariate ML model for the diagnosis of MDD (Figure 1). The largest MDD cohort to date will be used to assess the performance of these rs-FC classifiers at the individual level. Meanwhile, the relationships between rs-FC features and the severity of clinical symptoms in patients with MDD would be also explored.

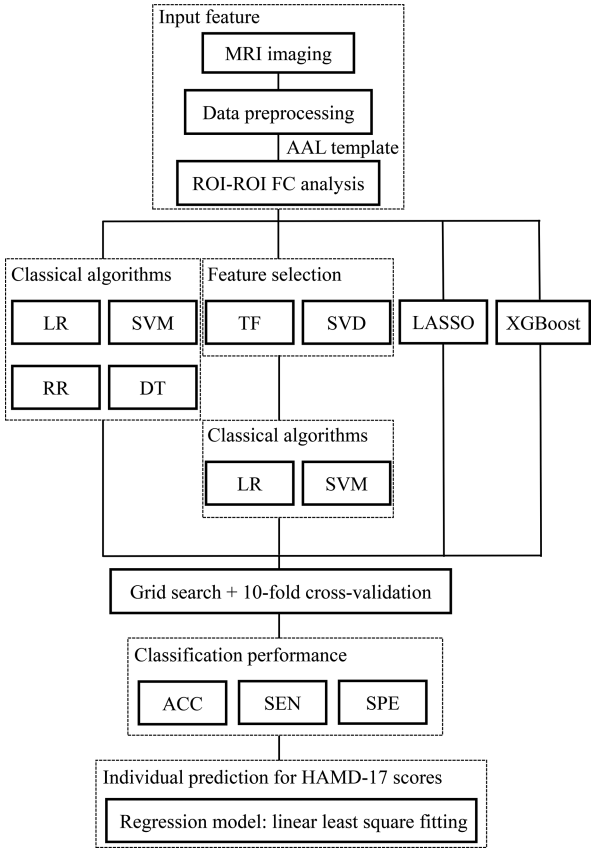

Figure 1. Study pipeline. MRI, magnetic resonance imaging; AAL, Automated Anatomical Labeling; ROI, regions of interest; LR, Logistics Regression; SVM, Support Vector Machine; RR Ridge Regression; DT, Decision Tree; TF, *t* test filter; SVD, Singular Value Decomposition; LASSO, Least Absolute Shrinkage and Selection Operator; XGBoost, eXtreme Gradient Boosting; ACC, accuracy; SEN, sensitivity; SPE, specificity; HAMD-17, 17 item Hamilton Depression Rating Scale.

RESULT

Sample Composition. Specifically, 1021 MDD patients and 1100 normal controls (NCs) were included in the present study for building ML classifiers. The clinical characteristics of these subjects were displayed in Table 1. There were significant differences in gender and education years between two groups, but no significant difference was observed in age. Among MDD patients, there were 478 patients with first-episode MDD and 197 patients with recurrent MDD; however, 346 patients were unclear for the episodicity status (first or recurrent) due to the data being unavailable.

Table 1. Clinical Characteristics of the Subjects[c]

variable	mean ± standard deviation MDD	NC	*P*-value
sample size	1021	1100	
age (years)	35.52 ± 13.40	36.18 ± 15.69	0.605[a]
gender (male/female)	336/685	460/640	<0.001[b]
education (years)	11.70 ± 3.74	12.24 ± 4.99	<0.001[a]
Number of First-Episode or Relapse			
first-episode	478		
relapse	197		
unknown	346		
Number of Subjects Obtaining Treatment			
drug-native	372		
treatment	349		
unknown	300		
HAMD-17 Scores			
	21.70 ± 5.99		

[a]Mann−Whitney U test. [b]Chi-square test. [c]MDD, major depressive disorder; NC, normal control; HAMD-17, 17 item Hamilton Depression Rating Scale.

Performances of the Classification Analysis. Figure 1 showed the whole workflow of ten classification procedures, and Figure 2 visualized the comparison of the performance of these classifiers for differentiating between MDD patients and NCs after controlling the age, gender, and education years. Among these classifiers, eXtreme Gradient Boosting (XGBoost) classifier showed the highest accuracy for distinguishing MDD patients from NCs [accuracy = 0.728, sensitivity = 0.720, specificity = 0.739, area under the curve (AUC) = 0.831; Table S2] and was identified as the optimal classifier. In addition, compared with Logistics Regression (LR) and SVM classifiers (LR: accuracy = 0.598, AUC = 0.628; SVM: accuracy = 0.637, AUC = 0.681; Table S2), the combined *t* test filter (TF) or Singular Value Decomposition (SVD) method with the LR or SVM algorithm can obtain an improved classification performance (TF+LR: accuracy = 0.624, AUC = 0.655; SVD+LR: accuracy = 0.657, AUC = 0.712; SVD+SVM: accuracy = 0.662, AUC = 0.724; SVD +SVM: accuracy = 0.689, AUC = 0.759; Table S2). However, the Least Absolute Shrinkage and Selection Operator (LASSO) algorithm did not show better classification performance between MDD patients and NCs based on the rs-FC data (accuracy = 0.643, AUC = 0.683; Table S2).

Identified rs-FC Features by the XGBoost Classifier. As the optimal model for the classification between MDD

https://doi.org/10.1021/acschemneuro.1c00256
ACS Chem. Neurosci. 2021, 12, 2878−2886

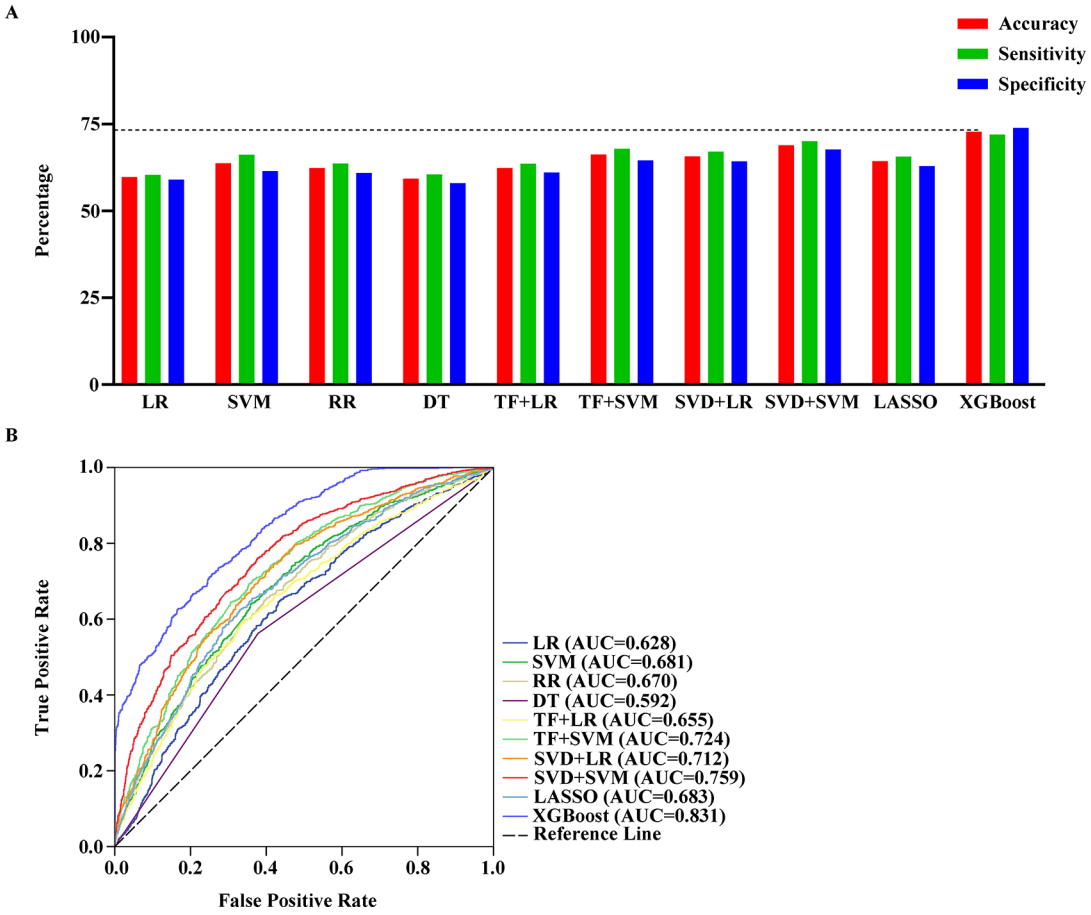

Figure 2. Classification results of multiple classifiers. (A) The accuracy, recall, and specificity of ten kinds of classifiers. (B) ROC curve of ten kinds of classifiers. LR, Logistics Regression; SVM, Support Vector Machine; RR Ridge Regression; DT, Decision Tree; TF, *t* test filter; SVD, Singular Value Decomposition; LASSO, Least Absolute Shrinkage and Selection Operator; XGBoost, eXtreme Gradient Boosting; ROC, receiver operating characteristic; AUC, area under the curve.

patients and NCs, 987 rs-FC features were identified in the XGBoost classifier. Among these features, the FC between the left inferior occipital gyrus and the right temporal pole showed the strongest weight values, followed by the connectivity between the right middle frontal gyrus and the right pallidum (Figure 3A). Meanwhile, after arranging 987 rs-FCs to 90 brain regions of the Automated Anatomical Labeling (AAL) atlas, the right orbital part of the middle frontal gyrus, the left fusiform gyrus, and the right superior occipital gyrus were associated with more than 30 rs-FCs (Figure 3B).

Furthermore, identified rs-FCs in the XGBoost classifier included 159 intranetwork FCs and 828 internetwork FCs, and these FCs were characterized by (1) most intranetwork FCs within the default mode network (DMN) (58 rs-FCs), followed by the limbic network (LN) (33 rs-FCs) and the visual network (VN) (28 rs-FCs) and (2) greater internetwork connectivity (>50 rs-FCs) comprised (i) between regions of DMN and LN, VN, sensorimotor network (SMN), and frontoparietal network (FPN); (ii) between regions of LN and VN; and (iii) between regions of VN and SMN (Figure 3C).

Linear Regression Analysis. The application of the linear regression model to the 987 rs-FC features of the XGBoost classifier allowed quantitative prediction of the 17 item Hamilton Depression Rating Scale (HAMD-17) scores with accuracy [multiple R^2 = 0.975, adjusted R^2 = 0.180, mean absolute error (MAE) = 0.739, root mean squared error (RMSE) = 0.946; Figure 4A]. The weight distribution of these rs-FC features for the regression model was displayed in Figure S1, and the top 50 features of the absolute weight were primarily associated with DMN (Figure 4B).

DISCUSSION

Using the large MDD data set, the present study compared rs-FC based classification among 10 ML classification algorithms and evaluated the effect of identified rs-FC features for the prediction of HAMD-17 scores in MDD patients. The results showed that (I) 4 commonly used ML algorithms [SVM, LR, Decision Tree (DT), and Ridge Regression (RR)] performed similarly poor rs-FC-based classification; however, the addition of the feature selection step (TF or SVD) can obviously improve the performance of using ML classification algorithms alone. (II) The LASSO algorithm (linear model) provided a nonideal discrimination with the high-dimensional rs-FC data, although the feature filtering process was also performed during the modeling period. (III) Compared with other models, the XGBoost method achieved the best classification performance between 1022 MDD patients and 1100 NCs. (IV) Frontal and occipital gyrus-related rs-FC features played an important role in the XGBoost classification, and rs-FC features identified by the XGBoost algorithm were primarily distributed within and between DMN, LN, and VN. (V) The HAMD-17 score can be predicted accurately for each MDD patient using rs-FC features of the XGBoost classifier. Taken

https://doi.org/10.1021/acschemneuro.1c00256
ACS Chem. Neurosci. 2021, 12, 2878−2886

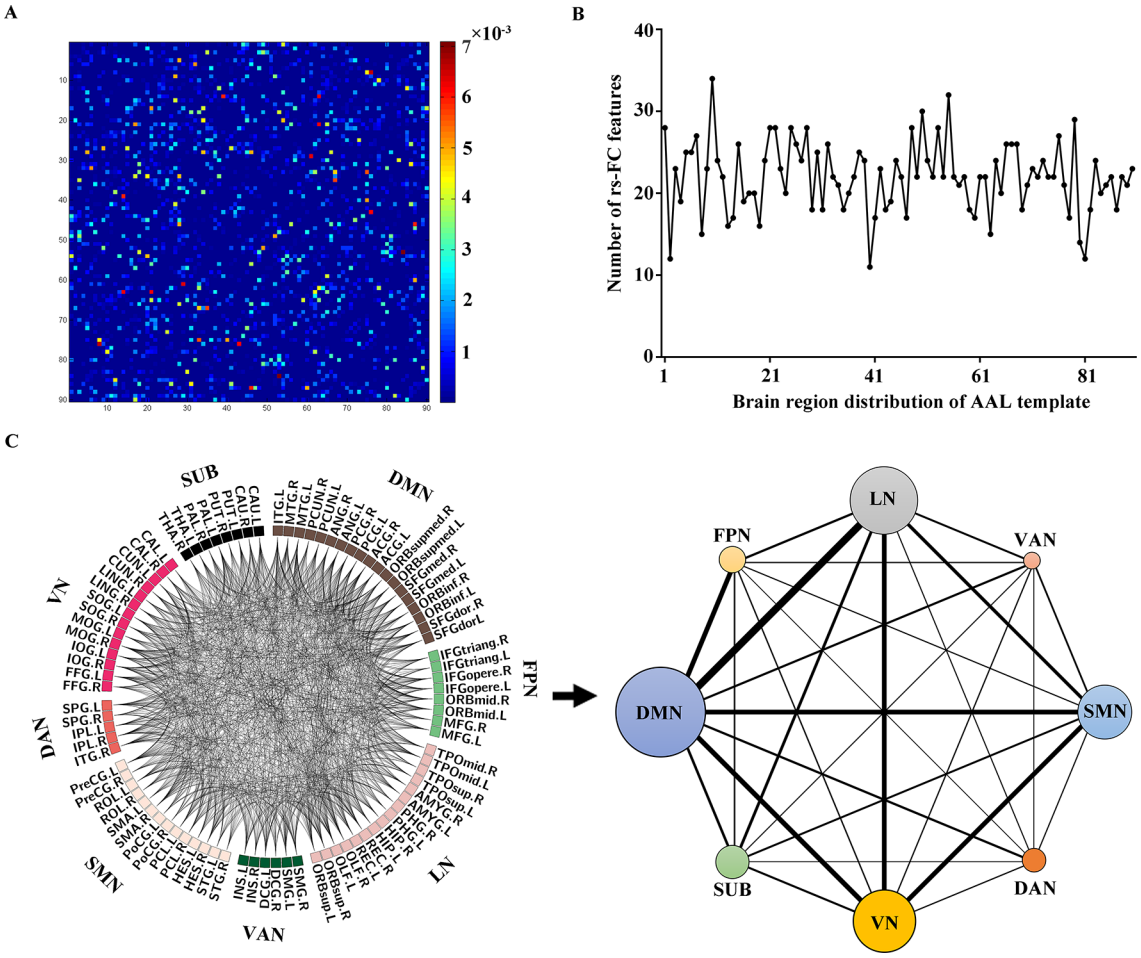

Figure 3. Features from the XGBoost classifier of whole-brain functional connectivity analysis using AAL template. (A) The weight of all features in the 90 × 90 matrix. The colored squares represent the present rs-FC features used in the classifier, and the darker the color, the greater the weight of the rs-FC feature. (B) The distribution of 987 rs-FC features of the classifier in 90 brain regions of AAL template. *X*-axis represents the sequence of brain regions of AAL template, and *Y*-axis represents the number of rs-FC at each node. (C) The distribution of 987 rs-FC features in 8 resting-state networks. In the left panel, the box in the ring represents brain regions, and the line connecting two boxes represents rs-FC of the two brain regions. Eight functional network modules are arranged to 90 brain regions, and these networks comprise functional connections linking different modules and connections within single modules. In the right panel, the rs-FC features within and between resting-state networks were visualized. Nodes with a larger size represent more rs-FCs within-network. Line width between nodes represents the number of rs-FCs of between-networks. XGBoost, eXtreme Gradient Boosting; rs-FC, resting-state functional connectivity; AAL, Automated Anatomical Labeling; DMN, default mode network; FPN, frontoparietal network; LN, limbic network; VAN, ventral attention network; SMN, sensorimotor network; DAN, dorsal attention network; VN, visual network; SUB, subcortical system.

together, the XGBoost classification model, based on rs-FC biomarkers reflecting the severity of the depressive symptom, can be used in the objective diagnosis of MDD.

Strictly progressive three-step ML analysis was used, after consideration of the high-dimensional problem and the interactive relationship between input features, to identify the optimal classification model (i.e., XGBoost model). The ensemble ML method is a combination of multiple simple algorithms, and the classification is achieved by a weighted vote among the simple classifiers.[14] XGBoost, one of the most commonly used ensemble methods, performs the classification by a weighted prediction among the trees, which can reduce classification bias and contribute to increasing the generalizability of the model.[15,16] In addition, compared with the Random Forest that is the other one commonly used ensemble method, the biggest advantage of XGBoost is its speed,[17] which suggests that the larger and more complex data set can be efficiently handled with less computational effort using XGBoost. Meanwhile, as a boosting method, XGBoost has the convenient parameter adjustment and can improve the prediction results by adding a new decision tree based on the existing trees, which is the other advantage.[18] While XGBoost had been successfully used in other classification tasks,[19,20] few studies were found to apply this method for the classification of MDD patients except for one study of functional near-infraredspectroscopy.[21] Therefore, in the present study, the XGBoost method was used excellently in the identification of MDD and showed good applicability for the high-dimensional rs-FC data.

Consistent with previous studies,[21,22] the present study demonstrated that XGBoost provided the best discrimination between two groups at the individual level as compared with other ML methods. In addition, frontal and occipital gyrus-related rs-FC features showed primary contribution for the XGBoost model, and the identified rs-FC features in the XGBoost classification model were distributed primarily within and between DMN, LN, and VN. Previous studies indicated that frontal regions participated in the reward-related

https://doi.org/10.1021/acschemneuro.1c00256
ACS Chem. Neurosci. 2021, 12, 2878−2886

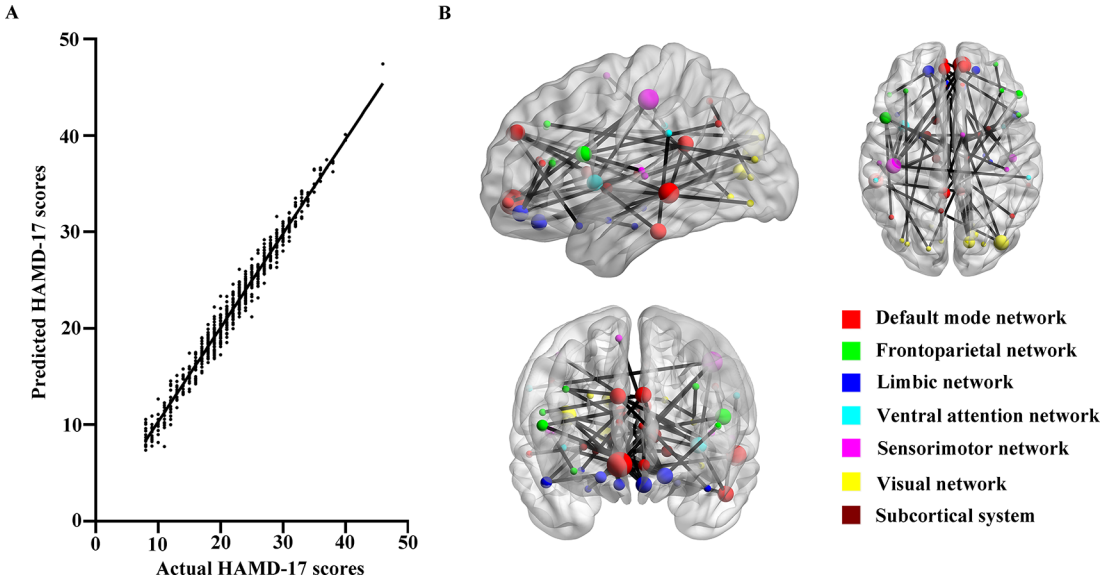

Figure 4. Linear regression analysis. (A) Scatter plot showing the predicted HAMD-17 scores for each subject and their actual HAMD-17 scores. Predicted score derived from 987 valid rs-FC features of the XGBoost classifier using linear regression model fitted by least-squares. (B) The distribution of the top 50 rs-FC features of the absolute weight score for the prediction model in the resting-state networks. The node with a larger size represents more rs-FCs related with the brain region. HAMD-17, 17 item Hamilton Depression Rating Scale; XGBoost, eXtreme Gradient Boosting; rs-FC, resting-state functional connectivity.

processing in MDD,[23] and the emotion-related regulation circuit comprised the fronto-limbic neural networks and DMN, whose abnormal function alterations were the primary characteristic of MDD.[24−26] In addition, dysfunctional DMN and LN connectivity patterns are not only associated with the identification of depression but are also valuable to guide individualized treatment strategies.[27−29] Furthermore, the primary visual cortex located in the occipital gyrus, can regulate the emotional processing via the amygdala and striatum,[30] which may be implicated in the MDD development. Meanwhile, the neural activity in the visual cortex may be a potential biomarker to predict the response to interventions in MDD, including antidepressant drugs[31,32] and repetitive transcranial magnetic stimulation.[33] More importantly, rs-FC features identified by the XGBoost can be used for the individual prediction of HAMD-17 scores in MDD patients, which further suggested that effective features of the XGBoost model were associated with the severity of the depressive symptom. Consequently, rs-FC data combined with the XGBoost method can provide an ideal classification performance in the diagnosis of MDD, and in the XGBoost model, identified rs-FCs within and between intrinsic brain networks may characterize the pathophysiology in MDD.

In the present study, data-driven ML approaches were used to make classifications from high-dimensional rs-FC data, and based on a multicentral, large-scale sample size, we proposed the XGBoost classification model for MDD with the better generalization and mechanistic interpretative. The current XGBoost classifier can achieve the accurate diagnosis of MDD patients at the personal level and be suitable to the high-dimensional neuroimaging data, which may be used as a convenient tool in the screening of MDD or a reliable diagnostic aid in the clinical practice of MDD. Although sex differences in emotion processing may play a role in inducing a difference of brain activity and women's increased risk for MDD,[34] the classification performances and identified rs-FC features of the male model, the female model, and the integrated model were similar (Figure S2), which further suggested that the present XGBoost model had better generalization and stability and could accurately diagnose MDD without being affected by sex differences.

The present study has several limitations. (I) Exclusively Chinese samples in the present multicentral databset may limit the generalization of the XGBoost classifier to other populations, and the UK Biobank database will be considered to test the current model in the subsequent study. (II) The detailed clinical information, such as the number of prior depressive episodes, negative life events, therapy details, and more neuropsychological assessments, was not provided for each MDD patient in some study sites, which limited our further analysis to explore the potential mechanism of the classification model and assess the classification performance in different MDD subtypes. (III) An inevitable issue of the multicentral data set is heterogeneity of MDD patients. Refining the homogeneity of subjects by using the single study site may improve the performance of the current classifier. Along this line, we selected the largest subdataset (S20 dataset) with 248 MDD patients and 251 NCs from the present multicentral dataset[35] to test the present XGBoost classifier. The accuracy of the classifier for the S20 dataset was 0.880 (sensitivity = 0.936, specificity = 0.825), and the AUC value was 0.944 (Figure S3), which suggested that the present XGBoost model showed the stronger discriminability and noninferiority classification performance when compared with previous studies with small samples (Table S1).

In conclusion, based on the high-dimensional rs-FC data, the XGBoost model showed the optimal classification performance between MDD patients and HCs, with good generalization, which suggested that rs-FCs have a diagnostic potential for MDD, and the XGBoost algorithm is a promising approach to achieve the individualized diagnosis of MDD. In addition, those rs-FCs identified by the XGBoost model can afford better neuroscientific interpretability for the pathophysiology of MDD.

https://doi.org/10.1021/acschemneuro.1c00256
ACS Chem. Neurosci. 2021, 12, 2878−2886

METHODS AND MATERIALS

Subjects. The REST-meta-MDD consortium is made up of different research groups across China and establish a multicenter, large-scale dataset that had been used in some previous studies.[28,35,36] The sample size that consisted of 1021 MDD patients and 1100 NCs from 24 study sites was used for analysis in the present study. The details on the inclusion and exclusion criteria can be found in the Supporting Information. All MDD patients met the Diagnostic and Statistical Manual of Mental Disorders IV criteria and underwent the HAMD-17 assessment. Each study site obtained approval from the local ethics committees, and all subjects or their legal guardians signed written consent forms. Clinical features of included subjects were displayed in Table 1.

MRI Data Preprocessing. Resting-state MRI data were acquired and preprocessed at each site using the Data Processing Assistant for Resting-State fMRI (http://www.restfmri.net/forum/dparsf) with a standard protocol,[37,38] which had been described in detail in previous studies[35,36] and the Supporting Information. Detailed MRI acquisition parameters for the different scanners were displayed in Table S3.

Whole-Brain FC Analysis. The AAL atlas, which is a widely used anatomical template including 78 cortical regions and 12 subcortical regions, was used to parcellate the cerebrum into 90 regions of interest (ROIs) (Table S4). The ROI-to-ROI FC analysis was performed using GRETNA (v2.0.0)[39] under the MATLAB environment (The MathWorks, Inc., Natick, MA, USA). The representative time series of each region was obtained by averaging the time series over all voxels in this region. Subsequently, the Pearson's correlation coefficients were computed in each possible ROI pair, and a Fisher's r-to-z transformation was performed for transforming the correlation coefficients to the z-score space, which can normalize the data to a standard normal distribution.[40] For each subject, a 90 × 90 matrix was obtained; then, the triangular portions of the matrix were extracted for transformation to a vectorial feature space with the 4005 dimensions.

ML Analysis. In the present study, a progressive three-step ML analysis was performed, including six different ML algorithms and two dimension reduction methods (Table S5). Details of these methods can be found in the Supporting Information. Python (ver3.7; www.python.org) was used for coding the algorithm. To make the results reproducible, all random seeds are recorded.

Step 1: Classical ML Algorithms. Four commonly used ML classification algorithms, including SVM, LR, DT, and RR, were performed for constructing the classification model based on the total 4005 rs-FCs features among all subjects, respectively.

Step 2: Feature Selection Combined With Classical ML Algorithms. For high-dimensional rs-FC data, the number of dimensions should be reduced to avoid the "curse of dimensionality".[41] The ML methods that were used in "Step 1", without an inherent feature selection ability, may be vulnerable to the high-dimensional data (Table S5). In the present study, two feature selection strategies (TF and SVD[42]) were applied to combine with LR and SVM algorithms for building a classification model, respectively. The introduction of dimension reduction techniques reduced the dimension of feature spaces from 4005 to 1000.

Step 3: Linear and Nonlinear ML Method. Linear ML methods may fail to perform the classification task based on the rs-FC data in consideration of the nonlinear relationship among input features.[43] In the present study, the LASSO,[44] a linear ML method, and the XGBoost,[16] a nonlinear ML method, were used to build a classification model, respectively. The inherent feature selection ability of these methods can contribute to achieving the dimension reduction for the rs-FC data (Table S5).

XGBoost Algorithm. XGBoost is an improved Gradient Boosted Decision Tree[45] algorithm designed for speed and performance, and the advantage of this method is to efficiently model nonlinear relationships in structural data. Briefly, this method repeatedly trains successive decision trees (weak learners) based on a set of the subject's FC features for constructing a combined strong classifier and generated an "overall score" to each subject for predicting the outcome. The derivations of objective function are as follows.

Supposing a data set of n samples and m features $D = \{(x_i, y_i)\}$ ($|D| = n$, $x_i \in R^m$, $y_i = \{0,1\}$), XGBoost will learn K decision trees and predict the output with their sum:

$$\hat{y}_i = \phi(x_i) = \sum_{k=1}^{K} f_k(x_i), f_k \in \mathcal{F}$$

where $\mathcal{F}$ is the space of the decision trees. To learn the set of decision trees used in XGBoost, we minimize the following regularized objective:

$$\mathcal{L}(\phi) = \sum_i l(y_i, \hat{y}_i) + \sum_k \Omega(f_k)$$

where $l(y_i, \hat{y}_i)$ is cross entropy and

$$\Omega(f) = \gamma T + \frac{1}{2}\lambda \|w\|^2$$

where T is the number of leaves in the tree and w is the leaf weight. XGBoost will start with a base tree classifier, which is a constant:

$$f_0(x) = argmin_c \sum_{i=1}^{n} l(y_i, c)$$

at the t-th iteration. XGBoost will need to add f_t to minimize the following objective:

$$\mathcal{L}^{(t)} = \sum_i [l(y_i, \hat{y}_i^{(t-1)} + f_t(x_i))] + \Omega(f_t)$$

which can be simplified as the following with second-order approximation:

$$\mathcal{L}^{(t)} \approx \sum_i \left[g_i f_t(x_i) + \frac{1}{2} h_i f_t^2(x_i) \right] + \Omega(f_t)$$

where g_i is the first-order derivative of $f_t(x_i)$ and h_i is the second-order derivative of $f_t(x_i)$.

Then, the loss function reduction given split is

$$\mathcal{L}_{\text{split}} = \frac{1}{2}\left[\frac{\left(\sum_{i\in I_L} g_i\right)^2}{\sum_{i\in I_L} h_i + \lambda} + \frac{\left(\sum_{i\in I_R} g_i\right)^2}{\sum_{i\in I_R} h_i + \lambda} - \frac{\left(\sum_{i\in I} g_i\right)^2}{\sum_{i\in I} h_i + \lambda} \right] - \gamma$$

With the above equation, the best split of the tree could be found by enumerates over all the possible splits, which is also known as the exact greedy algorithm. The whole algorithm for the XGBoost model was shown in Figure S4.

Furthermore, the parameters of XGBoost are restricted by L_1 norm, which results in the less informative features possibly being dropped during training; therefore, the XGBoost method is adaptive to the high-dimensional data set.

Hyper-Parameter Optimization and Cross-Validation. To obtain the optimum parameter sets of each ML method, the grid search was performed for the ML algorithm with fewer hyper-parameters. In addition, because the XGBoost algorithm included relatively complicated hyper-parameters (Table S6), an empirical strategy that achieves parameter tuning step-by-step was added and performed (Figure S4), and details were displayed in the Supporting Information.

Additionally, the 10-fold cross-validation was used to assess the generalization ability of various classifiers. In the process of cross-validation, samples were divided into 10 folds of equal size, and 9 folds were used for training; the remaining 1 fold was used as a test set. This process was performed for 10 rounds, and the average accuracy, sensitivity, and specificity were calculated to quantify the classification performance of models. Furthermore, the receiver operating characteristic curve was created by plotting the true positive rate against the false positive rate to measure the classification ability of the classifier. The AUC was used to reflect the performance of the classifier.

https://doi.org/10.1021/acschemneuro.1c00256
ACS Chem. Neurosci. 2021, 12, 2878−2886

Linear Regression Analysis. The relationship between clinical scores and rs-FCs was investigated using the linear regression analysis. Linear least-squares was used to fit the regression model for predicting the individual HAMD-17 score in MDD patients using the identified rs-FC features by the optimal classifier.

Assuming N features were retaining from the model, we performed a linear regression between the kept N features and HAMD-17 scores for the 1021 MDD patients, which can be formulated as

$$y = X\beta + \varepsilon$$

where X is 1021 × N feature matrix, y is 1021 × 1 response vector, and β is N × 1 coefficient vector. By least-squares approximation,[46] we want to minimize

$$\frac{1}{2}\sum_i (x_i\beta - y_i)^2$$

solving the objective function, we have

$$\hat{\beta} = (X^T X)^{-1} X^T y$$

The accuracy of the prediction model was evaluated with four frequently used statistics:[47−49] multiple R^2, adjusted R^2, MAE, and RMSE.

Network Analysis. To better interpret the performance of the optimal classifier, captured rs-FC features by the classifier would be further analyzed using a standard 7-system template.[50] As in our previous study,[51] the *priori* network modules for brain regions of the AAL atlas were defined; then, each AAL label (Table S4) was assigned to a matched functional system defined by Yeo et al.[50] In addition, subcortical regions were assigned to an eighth functional system named the subcortical module. As a result, the primary modular partition used in the present study included eight functional networks, i.e., DMN, FPN, LN, ventral attention network, SMN, dorsal attention network, VN, and subcortical system.

■ ASSOCIATED CONTENT

Supporting Information

The Supporting Information is available free of charge at https://pubs.acs.org/doi/10.1021/acschemneuro.1c00256.

Included information on REST-meta-MDD consortium data sets, image acquisition and data preprocessing, and detailed descriptions of each machine learning algorithm (PDF)

■ AUTHOR INFORMATION

Corresponding Authors

Deyu Zhou − *School of Computer Science and Engineering, Key Laboratory of Computer Network and Information Integration, Ministry of Education, Southeast University, Nanjing, Jiangsu 211189, China*; Email: d.zhou@seu.edu.cn

Zhijun Zhang − *Department of Neurology, Affiliated ZhongDa Hospital, School of Medicine, Institution of Neuropsychiatry, Southeast University, Nanjing, Jiangsu 210009, China; Shenzhen Institute of Advanced Technology, Chinese Academy of Sciences, Shenzhen, Guangdong 518055, China; School of Life Science and Technology, The Key Laboratory of Developmental Genes and Human Disease, Southeast University, Nanjing, Jiangsu 210009, China; Research Center for Brain Health, Pazhou Lab, Guangzhou, Guangdong 510330, China*; orcid.org/0000-0001-5480-0888; Phone: 86-025-83262241; Email: janemengzhang@vip.163.com; Fax: 86-25-83285132

Authors

Yachen Shi − *Department of Neurology, Affiliated ZhongDa Hospital, School of Medicine, Institution of Neuropsychiatry, Southeast University, Nanjing, Jiangsu 210009, China*

Linhai Zhang − *School of Computer Science and Engineering, Key Laboratory of Computer Network and Information Integration, Ministry of Education, Southeast University, Nanjing, Jiangsu 211189, China*

Zan Wang − *Department of Neurology, Affiliated ZhongDa Hospital, School of Medicine, Institution of Neuropsychiatry, Southeast University, Nanjing, Jiangsu 210009, China*; orcid.org/0000-0003-4770-2803

Xiang Lu − *Department of Neurology, Affiliated ZhongDa Hospital, School of Medicine, Institution of Neuropsychiatry, Southeast University, Nanjing, Jiangsu 210009, China*

Tao Wang − *School of Computer Science and Engineering, Key Laboratory of Computer Network and Information Integration, Ministry of Education, Southeast University, Nanjing, Jiangsu 211189, China*

Complete contact information is available at: https://pubs.acs.org/10.1021/acschemneuro.1c00256

Author Contributions

Y.S., L.Z., and Z.W. contributed equally to this work as shared first authors. Z.Z. and D.Z. were responsible for the study design. Y.S., L.Z., and Z.W. were responsible for data collection, data analysis, and writing the manuscript. X.L. and T.W. were responsible for the quality control of the study. Z.Zh., D.Z., and Y.S. were responsible for manuscript modification and discussion of the data analysis. All the authors have critically read the manuscript and approved the submitted version.

Notes

The authors declare no competing financial interest.

■ ACKNOWLEDGMENTS

This study was partly supported by the National Key Research and Development Plan of China (No. 2016YFC1306700), the National Natural Science Key Foundation of China (No. 81830040), the Science and Technology Program of Guangdong (No. 2018B030334001), the Program of Excellent Talents in Medical Science of Jiangsu Province (No. JCRCA2016006), and the National Natural Science Foundation of China (No. 81801680). We thank Miss. Cancan He, Miss. Xinyi Liu, Mr. Yao Zhu, and Miss. Qing Wang for their help in imaging data analysis. In addition, we are very grateful to the REST-meta-MDD Consortium (PIs: Prof. Chao-Gan Yan, Prof. Tian-Mei Si, Prof. Yan-Song Liu, Prof. Shu-Qian Yao, Prof. Xiang Wang, Prof. Wen-Bin Guo, Prof. Yi-Ru Fang, Prof. Dai-Hui Peng, Prof. Jun-Juan Zhu, Prof. Wei Chen, Prof. Fei Wang, Prof. Ying Wang, Prof. Ke-Rang Zhang, Prof. Qing-Hua Luo, Prof. Hua-Qing Meng, Prof. Qing-Hua Luo, Prof. Jian Yang, Prof. Xiao-Ping Wu, Prof. Guang-Rong Xie, Prof. Yong-Gui Yuan, Prof. Qi-Yong Gong, Prof. Kai-Ming Li, Prof. Li Kuang, Prof. Hong Yang, Prof. Kai Wang, Prof. Jiang Qiu, Prof. Chuan-Yue Wang, Prof. Zhe-Ning Liu, Prof. Tao Li, Prof. Xiu-Feng Xu, Prof. Yu-Qi Cheng, and Prof. Chunming Xie).

■ REFERENCES

(1) Otte, C., Gold, S. M., Penninx, B. W., et al. (2016) Major depressive disorder. *Nat. Rev. Dis Primers 2*, 16065.

(2) Malhi, G. S., and Mann, J. J. (2018) Depression. *Lancet 392* (10161), 2299−2312.
(3) Shi, Y., Luan, D., Song, R., and Zhang, Z. (2020) Value of peripheral neurotrophin levels for the diagnosis of depression and response to treatment: A systematic review and meta-analysis. *Eur. Neuropsychopharmacol. 41*, 40−51.
(4) Schatzberg, A. F. (2019) Scientific Issues Relevant to Improving the Diagnosis, Risk Assessment, and Treatment of Major Depression. *Am. J. Psychiatry 176* (5), 342−347.
(5) Gong, Q., and He, Y. (2015) Depression, neuroimaging and connectomics: a selective overview. *Biol. Psychiatry 77* (3), 223−235.
(6) Kaiser, R. H., Andrews-Hanna, J. R., Wager, T. D., and Pizzagalli, D. A. (2015) Large-Scale Network Dysfunction in Major Depressive Disorder: A Meta-analysis of Resting-State Functional Connectivity. *JAMA Psychiatry 72* (6), 603−611.
(7) Gong, L., Yin, Y., He, C., et al. (2017) Disrupted reward circuits is associated with cognitive deficits and depression severity in major depressive disorder. *J. Psychiatr. Res. 84*, 9−17.
(8) He, Z., Lu, F., Sheng, W., et al. (2019) Functional dysconnectivity within the emotion-regulating system is associated with affective symptoms in major depressive disorder: A resting-state fMRI study. *Aust N Z. J. Psychiatry 53* (6), 528−539.
(9) Zeng, L. L., Shen, H., Liu, L., and Hu, D. (2014) Unsupervised classification of major depression using functional connectivity MRI. *Hum Brain Mapp 35* (4), 1630−1641.
(10) Bhaumik, R., Jenkins, L. M., Gowins, J. R., et al. (2017) Multivariate pattern analysis strategies in detection of remitted major depressive disorder using resting state functional connectivity. *Neuroimage Clin 16*, 390−398.
(11) Geng, X., Xu, J., Liu, B., and Shi, Y. (2018) Multivariate Classification of Major Depressive Disorder Using the Effective Connectivity and Functional Connectivity. *Front. Neurosci. 12*, 38.
(12) Craddock, R. C., Holtzheimer, P. E., 3rd, Hu, X. P., and Mayberg, H. S. (2009) Disease state prediction from resting state functional connectivity. *Magn. Reson. Med. 62* (6), 1619−1628.
(13) Nascimento, D. S. C., Coelho, A. L. V., and Canuto, A. M. P. (2014) Integrating complementary techniques for promoting diversity in classifier ensembles: A systematic study. *Neurocomputing 138*, 347−357.
(14) Xia, Y., Liu, C., Li, Y., and Liu, N. (2017) A boosted decision tree approach using Bayesian hyper-parameter optimization for credit scoring. *Expert Systems with Applications 78*, 225−241.
(15) Fan, J., Yue, W., Wu, L., et al. (2018) Evaluation of SVM, ELM and four tree-based ensemble models for predicting daily reference evapotranspiration using limited meteorological data in different climates of China. *Agricultural and Forest Meteorology 263*, 225−241.
(16) Chen, T. Q., and Guestrin, C. (2016) Assoc Comp M. In *XGBoost: A Scalable Tree Boosting System*.
(17) Sheridan, R. P., Wang, W. M., Liaw, A., Ma, J., and Gifford, E. M. (2016) Extreme Gradient Boosting as a Method for Quantitative Structure-Activity Relationships. *J. Chem. Inf. Model. 56* (12), 2353−2360.
(18) Zhang, W. G., Wu, C. Z., Zhong, H. Y., Li, Y. Q., and Wang, L. (2021) Prediction of undrained shear strength using extreme gradient boosting and random forest based on Bayesian optimization. *Geosci. Front. 12* (1), 469−477.
(19) Suh, C. H., Shim, W. H., et al. (2020) Development and Validation of a Deep Learning-Based Automatic Brain Segmentation and Classification Algorithm for Alzheimer Disease Using 3D T1-Weighted Volumetric Images. *AJNR Am J Neuroradiol. 41* (12), 2227−2234.
(20) Tahmassebi, A., Wengert, G. J., Helbich, T. H., et al. (2019) Impact of Machine Learning With Multiparametric Magnetic Resonance Imaging of the Breast for Early Prediction of Response to Neoadjuvant Chemotherapy and Survival Outcomes in Breast Cancer Patients. *Invest. Radiol. 54* (2), 110−117.
(21) Zhu, Y., Jayagopal, J. K., Mehta, R. K., et al. (2020) Classifying Major Depressive Disorder Using fNIRS During Motor Rehabilitation. *IEEE Trans Neural Syst. Rehabil Eng. 28* (4), 961−969.
(22) Ruan, Y., Bellot, A., Moysova, Z., et al. (2020) Predicting the Risk of Inpatient Hypoglycemia With Machine Learning Using Electronic Health Records. *Diabetes Care 43* (7), 1504−1511.
(23) Zhang, W. N., Chang, S. H., Guo, L. Y., Zhang, K. L., and Wang, J. (2013) The neural correlates of reward-related processing in major depressive disorder: a meta-analysis of functional magnetic resonance imaging studies. *J. Affective Disord. 151* (2), 531−539.
(24) Zhong, X., Pu, W., and Yao, S. (2016) Functional alterations of fronto-limbic circuit and default mode network systems in first-episode, drug-naïve patients with major depressive disorder: A meta-analysis of resting-state fMRI data. *J. Affective Disord. 206*, 280−286.
(25) Du, L., Zeng, J., Liu, H., et al. (2017) Fronto-limbic disconnection in depressed patients with suicidal ideation: A resting-state functional connectivity study. *J. Affective Disord. 215*, 213−217.
(26) Etkin, A., Egner, T., and Kalisch, R. (2011) Emotional processing in anterior cingulate and medial prefrontal cortex. *Trends Cognit. Sci. 15* (2), 85−93.
(27) Drysdale, A. T., Grosenick, L., Downar, J., et al. (2017) Resting-state connectivity biomarkers define neurophysiological subtypes of depression. *Nat. Med. 23* (1), 28−38.
(28) Liang, S., Deng, W., Li, X., et al. (2020) Biotypes of major depressive disorder: Neuroimaging evidence from resting-state default mode network patterns. *Neuroimage Clin 28*, 102514.
(29) Korgaonkar, M. S., Goldstein-Piekarski, A. N., Fornito, A., and Williams, L. M. (2020) Intrinsic connectomes are a predictive biomarker of remission in major depressive disorder. *Mol. Psychiatry 25* (7), 1537−1549.
(30) Yu, C., Sellers, K. K., Radtke-Schuller, S., et al. (2016) Structural and functional connectivity between the lateral posterior-pulvinar complex and primary visual cortex in the ferret. *Eur. J. Neurosci 43* (2), 230−244.
(31) Furey, M. L., Drevets, W. C., Hoffman, E. M., Frankel, E., Speer, A. M., and Zarate, C. A., Jr. (2013) Potential of pretreatment neural activity in the visual cortex during emotional processing to predict treatment response to scopolamine in major depressive disorder. *JAMA Psychiatry 70* (3), 280−290.
(32) Keedwell, P., Drapier, D., Surguladze, S., Giampietro, V., Brammer, M., and Phillips, M. (2009) Neural markers of symptomatic improvement during antidepressant therapy in severe depression: subgenual cingulate and visual cortical responses to sad, but not happy, facial stimuli are correlated with changes in symptom score. *J. Psychopharmacol. 23* (7), 775−788.
(33) Zhang, Z., Zhang, H., Xie, C. M., et al. (2021) Task-related functional magnetic resonance imaging-based neuronavigation for the treatment of depression by individualized repetitive transcranial magnetic stimulation of the visual cortex. *Sci. China: Life Sci. 64* (1), 96−106.
(34) Jenkins, L. M., Kendall, A. D., Kassel, M. T., et al. (2018) Considering sex differences clarifies the effects of depression on facial emotion processing during fMRI. *J. Affective Disord. 225*, 129−136.
(35) Yan, C. G., Chen, X., Li, L., et al. (2019) Reduced default mode network functional connectivity in patients with recurrent major depressive disorder. *Proc. Natl. Acad. Sci. U. S. A. 116* (18), 9078−9083.
(36) Long, Y., Cao, H., Yan, C., et al. (2020) Altered resting-state dynamic functional brain networks in major depressive disorder: Findings from the REST-meta-MDD consortium. *Neuroimage Clin 26*, 102163.
(37) Chao-Gan, Y., and Yu-Feng, Z. (2010) DPARSF: A MATLAB Toolbox for "Pipeline" Data Analysis of Resting-State fMRI. *Front. Syst. Neurosci. 4*, 13.
(38) Yan, C. G., Wang, X. D., Zuo, X. N., and Zang, Y. F. (2016) DPABI: Data Processing & Analysis for (Resting-State) Brain Imaging. *Neuroinformatics 14* (3), 339−351.
(39) Wang, J., Wang, X., Xia, M., Liao, X., Evans, A., and He, Y. (2015) GRETNA: a graph theoretical network analysis toolbox for imaging connectomics. *Front. Hum. Neurosci. 9*, 386.

https://doi.org/10.1021/acschemneuro.1c00256
ACS Chem. Neurosci. 2021, 12, 2878−2886

(40) Park, J. E., Park, S. Y., Kim, H. J., and Kim, H. S. (2019) Reproducibility and Generalizability in Radiomics Modeling: Possible Strategies in Radiologic and Statistical Perspectives. *Korean Journal of Radiology 20* (7), 1124−1137.
(41) Kuo, F. Y., and Sloan, I. H. (2005) Lifting the curse of dimensionality. *Notices of the AMS 52* (11), 1320−1328.
(42) Stewart, G. W. (1993) ON THE EARLY HISTORY OF THE SINGULAR-VALUE DECOMPOSITION. *SIAM Rev. 35* (4), 551−566.
(43) Bohn, B., Garcke, J., and Iza-Teran, R.; et al. (2013) Analysis of car crash simulation data with nonlinear machine learning methods. In *International Conference on Computational Science* (Alexandrov, V., Lees, M., Krzhizhanovskaya, V., Dongarra, J., and Sloot, P. M. A., Eds.), Vol. *18*, pp 621−630.
(44) Tibshirani, R. (1996) Regression shrinkage and selection via the Lasso. *Journal of the Royal Statistical Society Series B-Methodological 58* (1), 267−288.
(45) Friedman, J. H. (2001) Greedy function approximation: A gradient boosting machine. *Annals of Statistics 29* (5), 1189−1232.
(46) Kamal, R., and Misra, S. (2019) Evaluation of Indian Prediction Models for Lung Function Parameters: A Statistical Approach. *Ann. Glob Health 85* (1), 21.
(47) Monnier, L., Mas, E., Ginet, C., et al. (2006) Activation of oxidative stress by acute glucose fluctuations compared with sustained chronic Hyperglycemia in patients with type 2 diabetes. *Jama-Journal of the American Medical Association 295* (14), 1681−1687.
(48) Adams, J. B., Audhya, T., McDonough-Means, S., et al. (2011) Nutritional and metabolic status of children with autism vs. neurotypical children, and the association with autism severity. *Nutr. Metab. 8*, 32.
(49) Tetko, I. V., Tanchuk, V. Y., and Villa, A. E. P. (2001) Prediction of n-octanol/water partition coefficients from PHYSPROP database using artificial neural networks and E-state indices. *J. Chem. Inf. Comput. Sci. 41* (5), 1407−1421.
(50) Yeo, B. T., Krienen, F. M., Sepulcre, J., et al. (2011) The organization of the human cerebral cortex estimated by intrinsic functional connectivity. *J. Neurophysiol. 106* (3), 1125−1165.
(51) Zhu, Y., Lu, T., Xie, C., et al. (2020) Functional Disorganization of Small-World Brain Networks in Patients With Ischemic Leukoaraiosis. *Front. Aging Neurosci. 12*, 203.

https://doi.org/10.1021/acschemneuro.1c00256
ACS Chem. Neurosci. 2021, 12, 2878−2886